Technical University of Denmark

DTU

Separation of foot-and-mouth disease virus leader protein activities; identification of mutants that retain efficient self-processing activity but poorly induce eIF4G cleavage

Belsham, Graham; Hua Guan, Su

DTU Library
Technical Information Center of Denmark

Separation of foot-and-mouth disease virus leader protein activities; identification of mutants that retain efficient self-processing activity but poorly induce eIF4G cleavage

Su Hua Guan and Graham J. Belsham*

Abstract

Foot-and-mouth disease virus is a picornavirus and its RNA genome encodes a large polyprotein. The N-terminal part of this polyprotein is the leader protein, a cysteine protease, termed L^{pro}. The virus causes the rapid inhibition of host cell cap-dependent protein synthesis within infected cells. This results from the L^{pro}-dependent cleavage of the cellular translation initiation factor eIF4G. L^{pro} also releases itself from the virus capsid precursor by cleaving the L/P1 junction. Using site-directed mutagenesis of the L^{pro} coding sequence, we have investigated the role of 51 separate amino acid residues in the functions of this protein. These selected residues either are highly conserved or are charged and exposed on the protein surface. Using transient expression assays, within BHK-21 cells, it was found that residues around the active site (W52, L53 and A149) of L^{pro} and others located elsewhere (K38, K39, R44, H138 and W159) are involved in the induction of eIF4G cleavage but not in the processing of the L/P1 junction. Modified viruses, encoding such amino acid substitutions within L^{pro}, can replicate in BHK-21 cells but did not grow well in primary bovine thyroid cells. This study characterizes mutant viruses that are deficient in blocking host cell responses to infection (e.g. interferon induction) and can assist in the rational design of antiviral agents targeting this process and in the production of attenuated viruses.

INTRODUCTION

Foot-and-mouth disease (FMD) is one of the most feared diseases of livestock animals. It is caused by FMD virus (FMDV), which can infect more than 70 different species including cattle, swine and sheep [1]. The disease can significantly impact the economy of affected countries [2]. FMDV is the prototypic member of the genus *Aphthovirus* within the family *Picornaviridae*. The genome of FMDV is a positive-sense, single-stranded RNA of about 8400 nucleotides (nt) and in the virus particle the viral RNA is enclosed within a protein shell (capsid) that includes 60 copies of each of the four structural proteins VP1, VP2, VP3 and VP4 [3].

The genome includes a single, large, open reading frame (ORF), circa 7000 nt, that encodes a polyprotein (circa 2330 residues). Translation of the RNA is initiated at two different AUG codons that are 84 nt apart, yielding two alternative forms of the N-terminal component of the polyprotein, namely the leader protease (L^{pro}); these are termed Lab (201 amino acids) and Lb (173 amino acids) [4, 5]. The 84 nt

spacer region (encoding 28 amino acids) is not required for virus viability but could have a role that is separate from its coding function, since deletion of the entire Lab sequence is not tolerated, whereas viruses lacking the 84 nt spacer region alone or the complete Lb coding sequence are viable within baby hamster kidney cells (BHK-21) [6]. Both forms of L^{pro} are identical at their C-termini and appear to display the same functions [7]. L^{pro} cleaves itself from the nascent capsid protein precursor P1-2A [8]. In addition, L^{pro} also induces the cleavage of the two homologues of a host cell translation initiation factor, termed eIF4GI [9] and eIF4GII [10]; these are around 46 % identical. This cleavage separates the N-terminal domain of eIF4G, which is responsible for attachment to the cap-binding protein eIF4E, from the rest of the molecule. This process results in the shut-off of host cell cap-dependent mRNA translation, a common hallmark of picornavirus infection [11]. In contrast, the initiation of translation on picornavirus RNA is achieved through a cap-independent mechanism directed by an internal ribosomal entry site (IRES) located within the 5′-untranslated region (UTR) and this process is maintained

following cleavage of eIF4G (e.g. see [11, 12]). FMDV 3C[pro] has also been shown to induce cleavage of eIF4G [13], at least in cells from certain species (e.g. BHK-21). This occurs on the C-terminal side of the site generated by the expression of the L[pro] and this cleavage occurs after the L[pro]-mediated cleavage is complete (see [14]). Cleavage of eIF4GI induced by L[pro] can be observed even in the absence of virus replication, when virus protein expression is very low [13]. Besides the FMDV protease, the L[pro] of other members of the genus *Aphthovirus*, namely bovine rhinitis B virus (BRBV) and equine rhinitis A virus (ERAV), also induce eIF4G cleavage [15, 16].

In addition to these activities, the FMDV L[pro] has also been reported to inhibit NF-κB activation [17] and to exhibit deubiquitinase (DUB) activity for certain critical signalling proteins of the type I interferon (IFN) signalling pathway [18]. Modification of the I83AL86A motif within a SAP (for SAF-A/B, Acinus, and PIAS) domain of L[pro] has been reported to abrogate the DUB activity as well as its ability to block signalling to the IFN-β promoter [18].

L[pro] is a papain-like cysteine proteinase with a flexible C-terminal extension (CTE) of 18 amino acid residues (Asp184-Lys201); the three-dimensional (3D) structure of the FMDV Lb[pro] has been determined [19]. The critical active site residues are Cys51 and His148 [20, 21]. Substitution of either of these residues ablates the L[pro] catalytic activities. The L/P1 cleavage site is well characterized; cleavage occurs at either a K/G or R/G junction (in different strains of FMDV, see [22]) and the cleavage can occur *in trans* [7] but also probably *in cis*. In contrast, the cleavage sites within the two distinct forms of eIF4G (eIF4GI and eIF4GII) are less well understood. Studies with eIF4GI identified a cleavage site produced *in vitro* by purified, recombinant, L protease as ANLG/RTTL [23]; however later studies on the closely related eIF4GII identified a cleavage site as LNVG/SRRS [10]. This cleavage site is not in the equivalent position to that in eIF4GI. It is possible that the cleavage of eIF4GI and eIF4GII occurs through an indirect mechanism (i.e. mediated by another protease, see [24]). Another cellular protein, Gemin5, has also been shown to be cleaved in the presence of the FMDV L[pro] [25]. Whatever the mechanism, it is apparent that the recognition of the cellular protein substrates by the FMDV L[pro] has to be significantly different from the recognition of the L/P1 junction within the viral polyprotein. Indeed, there is evidence that cleavage of the L/P1 junction *in vitro* can be affected without impact on eIF4G processing, and vice versa. Mutations Y168F and D163N clearly slowed the self-processing activity at the L/P1 junction but not eIF4G cleavage in cell-free extracts [26]. In contrast, deletion of the CTE or the presence of a modified C-terminus (L[pro]+9) greatly slowed the induction of eIF4G cleavage but these modifications do not affect the ability of mutants to process the polyprotein substrate *in vitro* [27]. Thus, it should, in principle, be possible to define specific features (i.e. individual amino acid residues)

of the L[pro] that differentially affect the cleavage of the distinct cellular and viral protein substrates within cells.

It has been shown that the sequence between two initiation codons of L[pro] is not essential for its cleavage functions [6, 7]. Therefore, the coding region of Lb was chosen as the target for mutational analysis in this study. Despite sharing protease activities, only 44 % of the residues in Lb[pro] were invariant among about 100 different FMDV isolates representing each of the seven different serotypes [22]. Using site-directed mutagenesis of the FMDV cDNA, we have now substituted both surface exposed and conserved residues within Lb[pro] and examined the properties of the mutant proteins that were generated using transient expression assays within cells. Selected modifications were also analysed in the context of the infectious virus and the influence of these modifications on the replication of FMDV was determined.

RESULTS

Screening for amino acid substitutions that differentially affect activities of FMDV Lb[pro]

As indicated above, many residues within the Lb[pro] are variable between different strains of FMDV. To identify residues that modify the substrate specificity of the L[pro], the conserved amino acids and the hydrophilic residues that are exposed to the aqueous solvent on the protein were located using the known 3D structure [19]. Codons corresponding to the selected residues were modified, using site-directed mutagenesis of cDNA including the L/VP4 coding region. In total, mutations encoding 51 different amino acid substitutions (out of 173 residues in Lb) were made (Fig. 1, Table 1).

As an initial screen, to analyse the properties of the mutant Lb proteins, BHK-21 cells [infected with the recombinant vaccinia virus vTF7-3, which expresses the T7 RNA polymerase (see [28])], were transfected with the mutant L[pro] expression plasmids together with a dicistronic luciferase reporter plasmid (pFluc/EMCV/Rluc, [29]). This plasmid expresses a dicistronic mRNA that encodes both firefly luciferase (Fluc) and *Renilla* luciferase (Rluc). The production of the latter is dependent on the activity of the IRES while the Fluc expression is achieved by cap-dependent translation initiation. The ratio of Fluc to Rluc activity observed in the presence of the catalytically inactive C51A mutant was set to 100 % and the relative levels of Fluc in the presence of the other forms of Lb were calculated and are shown in Table 1. The C51A mutant is modified at one of the two critical active site residues within L[pro] [20]. Wild-type (wt) L[pro], which induces eIF4G cleavage, strongly inhibited (to about 10 % of that seen with the C51A mutant) the cap-dependent expression of Fluc, as expected. In contrast, 19 mutant plasmids that were constructed in this study encoding the substitutions K38EK39E, K38EK39T, W52A, L53S, Q58EL59A, Q58E, A149D, G158AW159A, W159A, N46Q, D136A, D136AF137A, F137AH138A, H138P, V103AW105A, F151A, D164A, D163AD164AE165A and P182AD184AP187A within Lb[pro] had rather limited or

M N T T D C F I A L¹⁰ V Q A I R E I K A L²⁰ F L S R T T G K M E³⁰ L T L Y

N G E K K T⁴⁰ F Y S R P N N H D N⁵⁰ C* W L N A I L Q L F⁶⁰ R Y V E E P F

F D W⁷⁰ V Y S S P E N L T L⁸⁰ E A I K Q L E D L T⁹⁰ G L E L H E G G P P¹⁰⁰

A L V I W N I K H L¹¹⁰ L H T G I G T A S R¹²⁰ P S E V C M V D G T¹³⁰ D M C

L A D F H A G¹⁴⁰ I F L K G Q E H* A V¹⁵⁰ F A C V T S N G W Y¹⁶⁰ A I D D E

D F Y P W¹⁷⁰ T P D P S D V L V F¹⁸⁰ V P Y D Q E P L N G¹⁹⁰ E W K A K V Q R

K L K²⁰⁰ G

Fig. 1. The amino acid sequence of FMDV L^pro indicating targeted residues. The asterisks indicate the key catalytic residues (C51 and H148). Underlined residues are conserved among FMDV strains [22]. Residues in bold, italics were modified in this study. The sequence represents the complete Lab form of the protease; the Lb form lacks the N-terminal 28 amino acids.

no inhibitory effect on Fluc expression (similar to that observed with the mutant C51A, see Table 1). This indicates that these modifications abrogated the negative effect of L^pro on cap-dependent translation. In contrast, the other 35 mutants of Lb^pro produced a strongly negative impact on Fluc expression (less than 50 % of the Fluc activity seen with the C51A mutant, see Table 1).

To confirm and extend the analysis of the functionality of the L^pro mutants, the L/VP4 cleavage activity and the induction of eIF4GI cleavage within transfected BHK-21 cells were assessed for selected variants of the FMDV Lb. For these analyses, plasmids that express, from the T7 promoter, RNA transcripts containing the FMDV IRES (to maintain expression when eIF4G is cleaved) followed by the coding region for L/VP0 with a C-terminal FLAG epitope tag (termed L/VP0-FLAG) were used (Fig. 2a). Cells, infected with vTF7-3 as above, were transfected with the wt or mutant plasmids and cell extracts, prepared 20 h later, were analysed by immunoblotting using anti-eIF4GI and anti-FLAG antibodies. The properties of the mutant Lb proteins were compared to the wt protein and to the L^pro C51A mutant. As shown in Fig. 2(b), nearly all the tested mutant proteins (other than C51A) retained the L/VP4 self-cleavage activity since the FLAG-tagged VP0 was produced in each case. One exception was the Q58EL59A mutant, which had lost this function (n.b., in principle, the L/VP0 cleavage can occur either *in cis* or *in trans* in these assays since multiple copies of each mutant protein are made in the cells). Expression of the wt L^pro resulted in complete loss of the intact eIF4GI and the production of a specific cleavage product (Cp) whereas no loss of the intact eIF4GI was observed when the C51A mutant was expressed (Fig. 2c), as expected. Mutants K39E, R44A, N46Q, V103AW105G and F151A each induced quite high levels of eIF4GI cleavage but some residual intact protein was apparent. In contrast, only low levels of the eIF4GI Cp were observed with the mutants

K38EK39E, R44AH138A, W52A, L53S, Q58EL59A, A149D and W159A (Fig. 2c).

To test whether the mutations within the Lb coding region affect the L/VP0 cleavage *in trans*, the L^pro C51A-VP0 plasmid was co-transfected with two different amounts of the Lb^pro mutant plasmids. The plasmids tested were selected because each induced a very low level of eIF4GI cleavage activity in BHK-21 cells. The results (see Fig. 2d) showed that complete cleavage of the L/VP0 junction occurred with each of the mutants tested (except for C51A) when using the higher level of the plasmid. However, when a low level of the mutant Lb expression plasmid was used, then high levels of the uncleaved L/VP0 were observed for the W52A and L53S mutants and some precursor was also apparent with each of the other mutants tested as well (except for A149D). In contrast, L^pro C51A-VP0 was cleaved completely even in the presence of the low amount of wt L^pro plasmid (Fig.2d). Thus, these results showed the W52A and L53S amino acid substitutions impaired the *in trans* cleavage activity to some degree but did not block it completely, while the other selected mutants retained the ability to cleave the L/VP0 junction efficiently *in trans*.

Influence of the L^pro modifications on virus replication

To determine the importance of the modifications of L^pro activity in the context of the infectious virus, selected mutations (encoding the substitutions K38EK39E, R44AH138A, W52A, L53S, A149D and W159A) were introduced into the full-length cDNA of FMDV [strain O1 Kaufbeuren (O1K)]. Each of the variants selected retained the ability to cleave the L/VP0 junction; if this activity is lost it is highly unlikely that an infectious virus could be produced since this would prevent correct production of the virus capsid protein precursor P1-2A. Using these plasmids, full-length RNA transcripts were produced *in vitro* and then introduced into

Table 1. Effect of wt and mutant L^{pro} expression on cap-dependent translation in BHK-21 cells

The grey blocks indicate the modifications of Lb^{pro} that allow efficient cap-dependent translation of Fluc and were selected for further analysis. Data are presented as the mean±SD from the indicated number of independent experiments.

| Amino acid substitutions	Relative Fluc expression (%)	No. of observations
C51A	100	12
wt	10±2	6
K38A	17±2	3
K39E	34±4	3
K39A	36±9	3
K38AK39T	24±1	4
K38EK39T	66±11	3
K38EK39E	80±4	3
R44A	52±18	3
N46Q	63±13	3
D49A	25±11	3
W52A	96±5	3
L53S	97±6	3
L57A	21±10	3
Q58A	26±6	3
Q58E	79±13	3
L59A	38±5	4
Q58EL59A	93±12	3
R61T	27±8	3
D69A	24±7	3
E81A	22±10	3
K84A	23±9	3
D88A	20±14	3
D88AE96A	12±3	3
P99A	12±3	3
V103A	14±6	4
V103AW105G	92±13	3
K108A	19±7	3
T113A	19±6	3
R120A	19±5	3
P121A	30±2	3
E123A	19±5	3
D128A	39±10	3
G129A	25±7	3
L134A	35±6	3
D136A	87±11	3
H138P	92±8	3
D136AF137A	88±8	3
F137A H138A	78±13	3
E147A	15±2	3
E147AK144E	21±5	3
A149D	72±10	3
F151A	60±11	3
G158A	42±8	4
G158AW159A	92±8	3
W159A	99±2	3
D164A	95±7	3

Table 1. cont.

Amino acid substitutions	Relative Fluc expression (%)	No. of observations
E165A	21±11	3
D163AD164AE165A	100±0	3
P169AT171A	30±11	3
D173A	20±3	3
L178A	25±6	3
P187A	18±2	3
P182AD184AP187A	95±9	3
D184AE186A	44±2	3
L188A	22±4	3
E191AK193EK195A	20±5	3

BHK-21 cells by electroporation. As judged by the production of cytopathic effect (CPE) (passage 3), rescued viruses were obtained in each case. The virus stocks were titred and the presence of only the expected mutations within the L^{pro} coding sequence of the rescued viruses was confirmed by sequencing [following reverse transcription PCR (RT-PCR), data not shown]. The mutant viruses were then used to infect IBRS-2 cells (note in these cells, in contrast to BHK-21 cells, the FMDV 3C^{pro} does not induce eIF4G cleavage) [14]. Consistent with the results described above, the modifications to L^{pro} tested here had almost no impact on self-processing at the L/VP4 junction, as shown in Fig. 3(a), since VP0 (without L) was released from the polyprotein in each case.

As expected, with the wt L^{pro}, the cellular eIF4GI was largely cleaved at 2 h post infection (h.p.i.) and was completely processed at 4 h.p.i. In contrast, in uninfected cells or within cells infected with a mutant FMDV lacking the Lb coding region (ΔLb, [6]) the eIF4GI remained intact through to 6 h.p.i. The rescued viruses with just 1 or 2 amino acid substitutions within L^{pro} were much less efficient at producing eIF4G cleavage than the wt virus. Although some cleavage was detectable at 2 h.p.i. with mutants K38EK39E and A149D or at 4 h.p.i. (mutants R44AH138A, W52A, L53S, and W159A), intact eIF4GI persisted throughout the course of infection (up to 6 h.p.i.) for all of the mutants (Fig. 3b).

Time course of FMDV replication in pBTY cells

Primary bovine thyroid (pBTY) cells have been shown to be the most sensitive cell type for detecting field strains of all seven serotypes of FMDV [30]. However, as shown previously [6], the presence of a functional Lb protease is required for the virus to grow efficiently in pBTY cells. In this study, some CPE was observed in wt FMDV-infected pBTY cells at 10 h.p.i., and by 23 h.p.i. most of the monolayer was affected. In contrast, using the FMDV lacking the Lb coding region (ΔLb, [6]) and also the FMDVs with L^{pro} point mutants described above, >90 % of the pBTY cells were still unaffected visually by 23 h.p.i. However, in
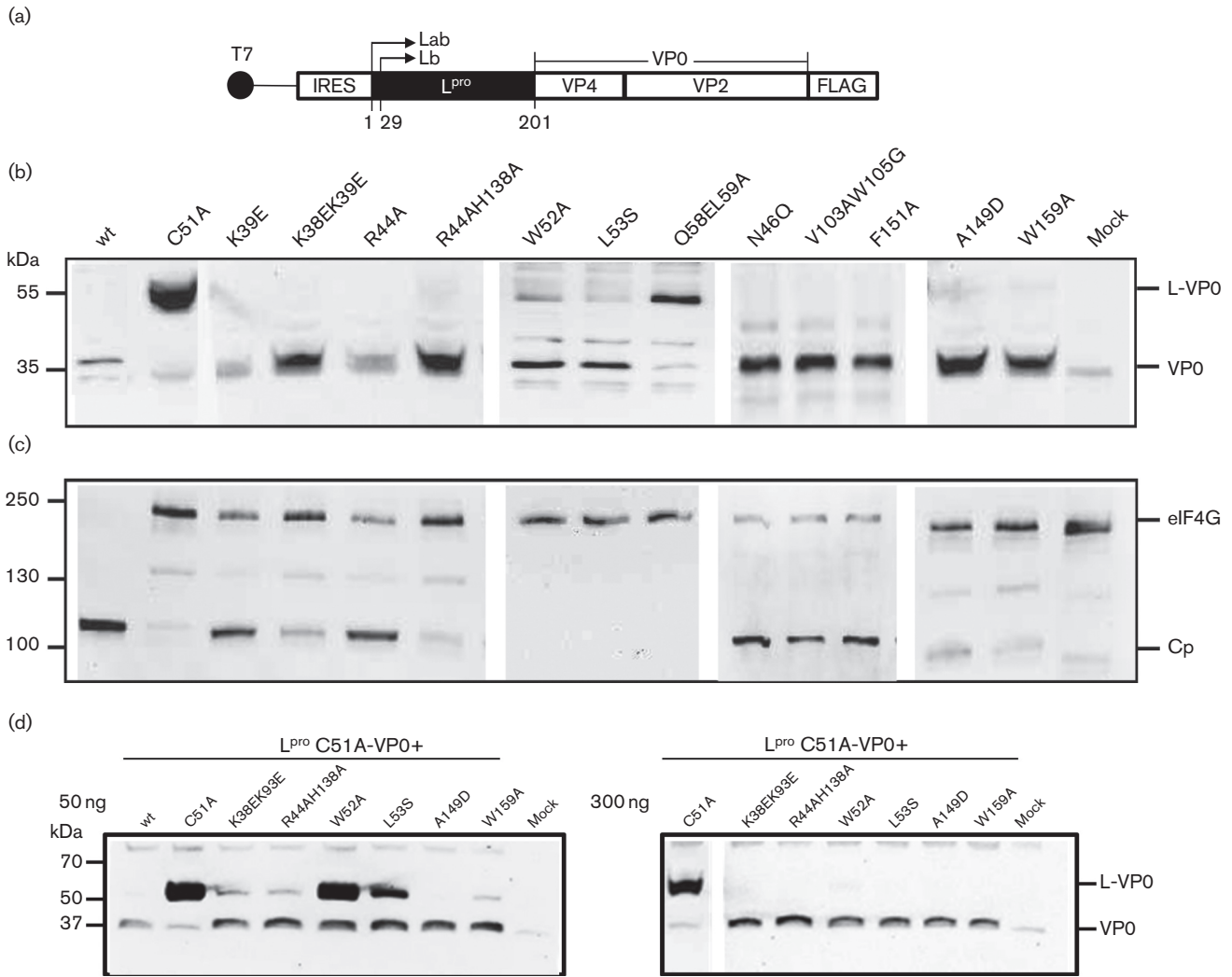
Fig. 2. Determination of L/VP0 and eIF4GI cleavage within BHK-21 cells expressing wt and mutant L^pro (a) Structure of the L^pro expressing plasmid. Fragments containing cDNA corresponding to the FMDV IRES upstream of the coding region for wt or mutated L^pro followed by VP0 and the FLAG epitope tag were inserted into pGEM-3Z, downstream of a T7 promoter, between *Eco*RI and *Bam*HI sites. (b) Cleavage of the L-VP0 junction by selected L^pro mutants. Cells, infected with vTF7-3, were transfected with the indicated plasmids and extracts were prepared 20 h later and analysed by SDS-PAGE and immunoblotting using an α-FLAG antibody. (c) Cleavage of eIF4GI induced by selected L^pro mutants. Samples prepared as described for panel (b) were analysed by immunoblotting using an α-eIF4GI antibody. The cleavage product of eIF4GI is indicated by Cp. (d) Effect of mutations on L^pro self-processing *in trans*. The L^pro C51A-VP0 plasmid was cotransfected with two different amounts (50 ng and 300 ng) of the indicated L^pro mutant plasmids. The extracts were prepared 20 h later and analysed by SDS-PAGE and immunoblotting using an α-FLAG antibody.

BHK-21 cells, each of the viruses (wt and mutants) induced 80–90 % CPE by 23 h.p.i. (data not shown).

To analyse, in more detail, the growth characteristics of the mutant O1K viruses, with just one or two amino acid substitutions in the L^pro, we infected, at low m.o.i. (0.01 TCID$_{50}$ cell^{-1}), both pBTY cells (Fig. 4a) and, in parallel, BHK-21 cells (Fig. 4b). The replication of each virus was measured using quantitative real-time RT-PCR (RT-qPCR) assays that determine the level of FMDV RNA within the samples collected at multiple time points after the start of the infection. In BHK-21 cells, each of the viruses grew with similar

kinetics but it was noted that by 10 h.p.i., the level of wt FMDV RNA accumulated to higher levels than for the L^pro mutants. As shown in Fig. 4(a), wt FMDV also grew well in pBTY cells. However, in contrast, little or no amplification of any of the L^pro mutant viruses was observed beyond 5 h. p.i. (Fig. 4a).

DISCUSSION

The 3D structure of Lb^pro includes an active site with the two key catalytic residues, C51 and H148, on the opposite sides of a cleft separating two domains, an α-helical
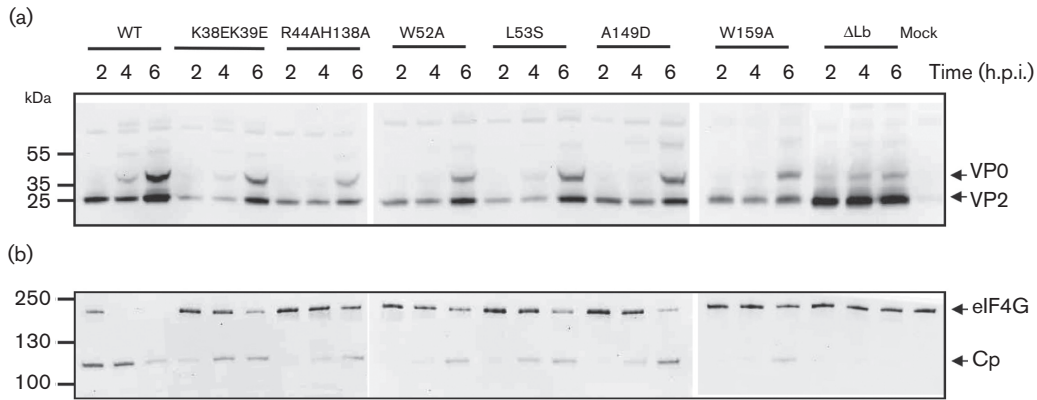
Fig. 3. Properties of wt and L^{pro} mutants within FMDV-infected IBRS-2 cells. IBRS-2 cells were infected with rescued wt or mutant FMDVs, as indicated, at an m.o.i. of 2. Cytoplasmic extracts were prepared at the indicated times post-infection and analysed by SDS-PAGE and immunoblotting. (a) L^{pro} self-processing at the L/P1 junction to produce VP0 was detected using an α-FMDV VP2 antibody. (b) eIF4GI cleavage induced by the expression of wt and mutant FMDV L^{pro} was detected using an α-eIF4GI antibody.

domain and β-sheet domain including the C-terminal region with a unique CTE (Fig. 5a). Residues 183–195 of the CTE have been shown to be important for the

Fig. 4. Growth curves for wt and mutant viruses in pBTY and BHK-21 cells. The rescued wt and mutant FMDVs, as indicated, were used to infect pBTY cells (a) or BHK-21 cells (b) at an m.o.i. of 0.01 TCID$_{50}$ cell^{-1}, and harvested after freezing from 0 to 23 h later. Total RNA was extracted and the level of FMDV RNA was measured using RT-qPCR assays and is expressed as RNA copies per ml of virus harvest. Results are representative of three separate experiments.

interaction with eIF4GI [27]. The Lb^{pro} with only a partial CTE (residues 183–195) retained the activities of wt Lb^{pro}, whereas deletion of the entire CTE reduced the ability to induce cleavage of eIF4G. Modification of residue C133, which is structurally clo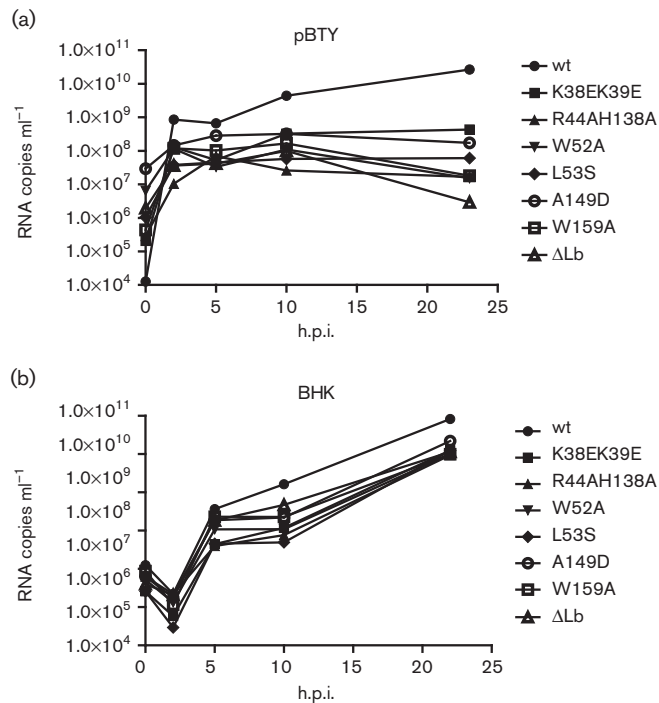se to the CTE, produced similar results *in vitro* [31]. Further study indicated that the conserved residues D184 and E186 within the CTE were important for this loss of function [32].

Some studies have indicated that the cleavage of eIF4G induced by the FMDV L^{pro} requires the interaction of eIF4G with the cap-binding protein eIF4E [33]; this translation initiation factor binds to the N-terminal region of eIF4G. Recent studies have shown that interaction of Lb^{pro} with a short fragment of eIF4GII requires the presence of eIF4E [34], within a heterotrimeric complex, and that residue C133 and the CTE of Lb^{pro} are required for the interaction with eIF4E. However, these experiments were based on the use of rabbit reticulocyte lysate (RRL) *in vitro* translation system and were focused on the CTE and residues around the active site. Here we have investigated the conserved and charged amino acid residues distributed across the surface of the L^{pro} structure and generated an insight into the roles of these residues in producing cleavage of eIF4G within cells.

Compared to other papain-like proteases, L^{pro} displays a deeper and narrower cleft (S1 subsite) with the active site at the bottom, the loop preceding the central helix α1 (N50–E61) on one side, and the β-turn connecting strands β5 and β6 (F137–S156) on the other [19]. Among the residues involved in this subsite, the amino acid substitutions W52A, L53S, Q58EL59A, and A149D each led to the loss of eIF4G cleavage activity (see Fig. 2c). The double mutant Q58EL59A also failed to release L^{pro} from the polyprotein. These key residues are all located in the vicinity of the active site (see Fig. 5a) and may contribute to the substrate
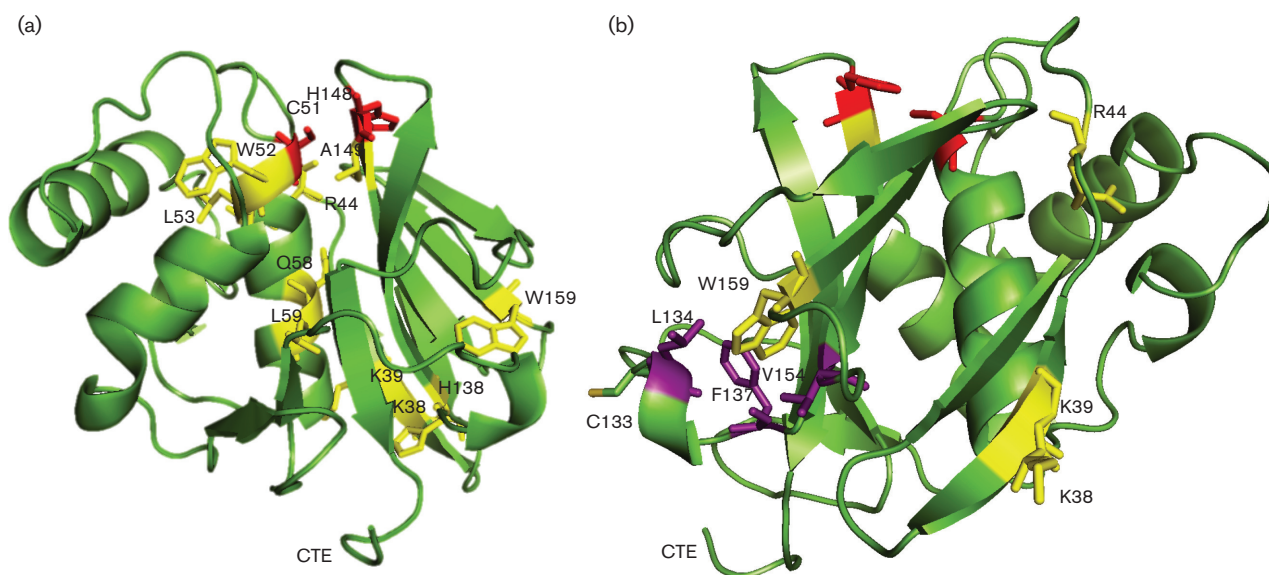
Fig. 5. Location of residues affecting induction of eIF4G cleavage. (a) 3D structure of Lb[pro] [19] (PDB ID code 1QOL, annotated using PyMol). The two critical active site residues (C51 and H148) are marked in red. Residues coloured yellow were demonstrated in this study to play an important role in eIF4GI cleavage. (b) Hydrophobic region. Residues in purple form a hydrophobic region with residue W159.

recognition since (apart from the double mutant) they do not affect the L/P1 cleavage activity; thus they do not affect the catalytic activity of the enzyme *per se*. It is noteworthy that these residues are highly conserved in FMDV [22] and they (except W52 and A149) are also present in the equivalent positions within the L protease of ERAV but not in the L[pro] of equine rhinitis B virus (ERBV) [16]. Unlike the ERBV L[pro], which is unable to shut down cellular cap-dependent translation, the ERAV L[pro] and FMDV L[pro] both induce cleavage of eIF4GI at very similar or identical positions [16]. Taken together, these observations are consistent with a significant role for these residues, around the S1 subsite, in the induction of eIF4G cleavage by L[pro].

Residues W52 and A149 are also involved in the S2 subsite, a deep hydrophobic pocket [19]. A comparison between the monomeric Lb[pro] L200F and sLb[pro] (lacking the last six residues of Lb[pro]) showed that residue W52 displayed a significant backbone amide shift when the C-terminal residues were removed [35], suggesting an interaction between W52 and the CTE. Moreover, W52 is adjacent to the catalytic residue C51. These properties may contribute to the loss of eIF4G cleavage observed with the mutant W52A; however the L/P1 cleavage activity was retained by this mutant so the enzyme is clearly still active (c.f. the C51A mutant). The conserved residue A149 is adjacent to the other key catalytic residue H148. Modification of A149 to the charged Asp (A149D) resulted in delayed eIF4G cleavage (Fig. 3b). This modification changes the hydrophobic environment and the acidic side chain of Asp may modify the space for the substrate to penetrate into the S2 pocket. Indeed, clear chemical

shifts were observed for residues involved in the S2 pocket in the presence of a 12 amino acid peptide derived from eIF4GI [36].

In this study, we have also shown the importance of residues K38, K39 and R44 for the Lb[pro]- induced cleavage of eIF4G. It seems that an acidic side chain (as in Glu, E) is not tolerated in place of K38 or K39. The double substitutions K38EK39E significantly impaired the cleavage of eIF4G (Fig. 3b, c). However, this was not the case for the single-point mutants K38A and K39A (n.b. these changes introduce a neutral amino acid rather than an acidic residue), which both significantly inhibited the expression of Fluc, reflecting loss of intact eIF4G (Table 1). It could be that the double substitutions K38AK39A would have a similar effect to K38EK39E on eIF4G cleavage induced by Lb[pro]. However, the mutant K38AK39T that has lost both the basic side chains impaired cap-dependent translation (as monitored by Fluc expression, see Table 1). The substitution K39E alone or in K38EK39T has a clear negative impact on Fluc expression (Table 1) and induced eIF4G processing albeit these effects were weaker than with the wt L[pro]. Therefore, it appears that the double substitutions in K38EK39E change the local ionic environment leading to a reduction in the L[pro]-induced eIF4G cleavage activity.

Amino acids R44 and H138 are conserved, charged residues within Lb. It is apparent from the 3D structure that, like K38 and K39, the side chain of R44 protrudes away from the globular domain of L[pro] (Fig. 5b) and none of these residues appears to interact with the CTE [19]. Instead, these basic side chains are well positioned to interact with

residues from another protein. However, the interaction may be not very strong or at least involve more than one residue. It is apparent that single mutants K39E and R44A did not reduce the eIF4G cleavage as much as the double mutants K38EK39E and R44AH138A. These results are consistent with previous observations that the mutant H138L was reduced in its ability to induce eIF4G cleavage but did not affect self-processing activity [21].

Residue W159 was investigated here due to its conservation in FMDV, BRBV and ERAV (data not shown). The modification W159A greatly decreased the eIF4G cleavage induced by L^{pro} compared to wt. The cleaved product could only be observed from 6 h.p.i. in virus-infected cells (Fig. 3b). The side chain of W159 together with residues L134, F137 and V154 form a very hydrophobic region within the structure of L^{pro} (Fig. 5b). Studies using NMR showed amide chemical shift changes for these residues in the presence of an eIF4GI-derived 12mer peptide [36], suggesting the possible involvement of these residues in substrate interaction. Indeed, as shown here, the substitutions in mutant D136AF137A resulted in the high cap-dependent expression of Fluc (Table 1) (i.e. reflecting poor eIF4G cleavage). From closer investigation of the 3D structure, it was found that in addition to the residues that are close to the active site (W52, L53 and A149), residues located on β-sheets (K39, R44, C133, F137, H138 and W159) form a surface-like region. Moreover, this region is highly conserved, indicating that this surface may play a significant role in the protein interactions required for cleavage of eIF4G.

Some of the mutants generated in this study have been shown to be tolerated within the context of infectious FMDV in BHK-21 cells but these mutant viruses have lost their ability to replicate well in pBTY cells. This may be due to their failure to induce eIF4G cleavage efficiently; consequently, the mutant FMDVs can be expected to fail to inhibit interferon production [37]. Thus these studies may facilitate the development of effective new strategies that target L^{pro} for the control of FMDV infection. Furthermore, the characterization of such mutant viruses can contribute to the development of engineered, attenuated viruses that can be grown, e.g. for vaccine antigen production, outside of high containment facilities.

METHODS

Construction of plasmids containing mutations in the Lb^{pro} coding region

The plasmid pT7S3 [38] contains the full-length cDNA for the O1Kaufbeuren B64 strain of FMDV. To modify the Lb^{pro} coding region, a *Kpn*I fragment (circa 1.4 kb) from pT7S3 was inserted into *Kpn*I-digested pGEM3Z (Promega), generating pSG2. The nucleotides encoding the targeted amino acids within the coding region of Lb^{pro} were modified by site-directed mutagenesis [39]. Briefly, fragments were amplified using pSG2 as template with forward primers carrying mutations (Table S1, available in the online Supplementary Material) and a reverse primer (SP6)

in separate PCRs. The amplicons were gel purified and used as megaprimers for the second round of amplifications again using pSG2 as the template. The PCR products were digested with *Dpn*I, to remove the template DNA, and then transformed into competent *E. coli*. Plasmid DNAs isolated from the resultant colonies were then sequenced using primers T7 and SP6 to confirm the presence of the expected mutations and the absence of other changes.

To facilitate the analysis of L/P1 cleavage activity, a FLAG-epitope tag was introduced at the C-terminus of the coding region for the VP2 capsid protein. Thus, the cDNA fragment corresponding to the IRES followed by the L/VP4/VP2 (L-VP0) coding region was amplified using primers SG1 and SG42 with the plasmid pT7S3 (as above) as template. The fragment (2007 bp) was digested with *Eco*RI and *Bam*HI and ligated into similarly digested pGEM3Z, generating pSG42. Individual mutations within the Lb coding region were introduced by site-directed mutagenesis and resulted in the following substitutions: C51A, W52A, L53S, K38EK39E, Q58EL59A, A149D and W159A (following the numbering system for the Lab form of L^{pro}). Briefly, primers 10PPN36 and SG57 (Table S1), and the derivatives of pSG2 carrying the mutations were used as the templates to generate megaprimers for the second round PCRs. The template in the second round of PCR was pSG42. The final constructs were sequenced throughout the L/VP2 coding region using primers SG1 and SG42.

Transient expression assays

Plasmid DNAs were transfected, using FuGene 6 (Promega) as described by the manufacturer, into BHK-21 cells (35 mm wells, circa 90 % confluent) that had been infected with the recombinant vaccinia virus vTF7-3 [28] which expresses the T7 RNA polymerase essentially as described [29]. For the luciferase assays, the pSG2 variants with mutations in Lb^{pro} (30 ng) were co-transfected with pFluc/EMCV/Rluc (2 µg) (this expresses both firefly and *Renilla* luciferase; [29]). Inhibition of cap-dependent translation was monitored by measuring Fluc expression relative to the Rluc expression. The cap-independent expression of the Rluc is directed by the EMCV IRES. At 20 h.p.i., cell lysates were prepared using the Rluc assay lysis buffer for Fluc and Rluc assays, or using buffer C [20 mM Tris-HCl (pH 8.0), 125 mM NaCl, and 0.5 % NP-40] for Western blot analysis, and extracts were clarified by centrifugation at 18 000 g for 10 min at 4 °C.

Luciferase reporter assays

Fluc and Rluc activities were determined using the firefly and *Renilla* reporter assay systems (Promega), respectively, according to the manufacturer's protocol. The Fluc activities were normalized to the measured Rluc activities and the data were collected from at least three independently conducted experiments.

Immunoblotting

Immunoblotting was performed according to standard methods as described previously [40]. Briefly, samples were

mixed with 2× Laemmli sample buffer (containing 25 mM DTT), separated by SDS-PAGE (4–15 % polyacrylamide from Bio-Rad), and transferred to PVDF membranes (Millipore). After blocking in 5 % nonfat dry milk and 0.1 % Tween 20 in PBS, membranes were incubated with primary antibodies diluted in the same buffer. The following primary antibodies were used as described [41]: monoclonal mouse anti-FLAG 1 : 3000 dilution (Sigma); polyclonal rabbit anti-eIF4GI (1 : 2000 dilution, kindly provided by N. Sonenberg, McGill University, Montreal, Canada, diluted in 5 % BSA); and anti-FMDV VP2 1 : 2000 (mouse monoclonal antibody 4B2, kindly provided by L. Yu, Harbin, P. R. China). Bound proteins were visualized using the appropriate secondary, horseradish peroxidase-conjugated antibodies (Dako). Detection was achieved using chemiluminescence reagents (Pierce ECL; Thermo Fisher Scientific) and images were captured using a Chemi-Doc XRS system (Bio-Rad).

Rescue of viruses from full-length FMDV cDNA

To introduce mutations into the FMDV full-length cDNA, the *Kpn*I fragment from the pSG2-derived plasmids was ligated to *Kpn*I-digested pT7S3-*Nhe*I [42]. The presence of the mutations was confirmed by sequencing using primers 10PPN36 and SG57 (Table S1). The plasmids containing the wt and mutant full-length FMDV cDNAs were linearized by digestion with *Hpa*I, then purified (Fermentas PCR purification kit), and *in vitro* transcribed using T7 RNA polymerase (Megascript kit; Ambion) as described by the manufacturer. The RNA transcripts were analysed using agarose gel electrophoresis and then introduced into BHK-21 cells by electroporation as described previously [43] and incubated at 37 °C for 48 h. The viruses were harvested following freezing, and amplified in one or two subsequent passages (P2 or P3) in BHK-21 cells. The appearance of cytopathic effect (CPE) was monitored during each passage. After these passages, when CPE was apparent, viral RNA was extracted (QIAamp RNA Blood Mini kit; Qiagen) and reverse transcribed using Ready-To-Go You-Prime First-Strand Beads (GE Healthcare, Life Sciences), and amplicons (900 bp) corresponding to the L/VP4 coding region were amplified by PCR using primers 10PPN36 and SG57 (Table S1). The products were sequenced to confirm the presence of the introduced mutations. Note that control reactions, lacking reverse transcriptase, were used to show that the PCR products obtained were derived from the viral RNA template. Viral titres were determined, as 50 % tissue culture infectious doses (TCID$_{50}$), by titration in BHK-21 cells, according to standard procedures [44].

Infection and virus growth kinetics

BHK-21, IBRS-2 and pBTY cells were grown in Dulbecco's modified Eagle's medium supplemented with 5 (BHK-21 and IBRS-2) or 1 % (pBTY) foetal bovine serum. Cells were infected with either wt or mutant FMDV. After a 1 h adsorption step, additional medium was added and the infection was left to progress and stopped at pre-selected times. For immunoblotting analysis, IBRS-2 cells were

infected at an m.o.i. of 2. Cells were harvested at selected times with buffer C (as above).

For virus growth kinetics, BHK-21 and pBTY cells were infected at an m.o.i. of 0.01 at 37 °C. Infections were stopped at selected times by freezing. Viral RNA was isolated using a robotic protocol (MagNA Pure LC Total Nucleic Acid Isolation kit, Roche) as described by the manufacturer and the RNA samples were eluted in 50 µl of water. The production of FMDV RNA was determined using RT-qPCR as described previously [45, 46].

References
1. **Jamal SM, Belsham GJ.** Foot-and-mouth disease: past, present and future. *Vet Res* 2013;44:116.
2. **Pattnaik B, Subramaniam S, Sanyal A, Mohapatra JK, Dash BB** *et al.* Foot-and-mouth disease: global status and future road map for control and prevention in India. *Agric Res* 2012;1:132–147.
3. **Belsham GJ.** Translation and replication of FMDV RNA. *Curr Top Microbiol Immunol* 2005;288:43–70.
4. **Beck E, Forss S, Strebel K, Cattaneo R, Feil G.** Structure of the FMDV translation initiation site and of the structural proteins. *Nucleic Acids Res* 1983;11:7873–7885.
5. **Clarke BE, Sangar DV, Burroughs JN, Newton SE, Carroll AR** *et al.* Two initiation sites for foot-and-mouth disease virus polyprotein *in vivo*. *J Gen Virol* 1985;66:2615–2626.
6. **Belsham GJ.** Influence of the leader protein coding region of foot-and-mouth disease virus on virus replication. *J Gen Virol* 2013;94: 1486–1495.
7. **Medina M, Domingo E, Brangwyn JK, Belsham GJ.** The two species of the foot-and-mouth disease virus leader protein, expressed individually, exhibit the same activities. *Virology* 1993; 194:355–359.
8. **Strebel K, Beck E.** A second protease of foot-and-mouth disease virus. *J Virol* 1986;58:893–899.
9. **Devaney MA, Vakharia VN, Lloyd RE, Ehrenfeld E, Grubman MJ.** Leader protein of foot-and-mouth disease virus is required for cleavage of the p220 component of the cap-binding protein complex. *J Virol* 1988;62:4407–4409.
10. **Gradi A, Foeger N, Strong R, Svitkin YV, Sonenberg N** *et al.* Cleavage of eukaryotic translation initiation factor 4GII within foot-and-mouth disease virus-infected cells: identification of the L-protease cleavage site *in vitro*. *J Virol* 2004;78:3271–3278.
11. **Belsham GJ, Jackson RJ.** Translation initiation on picornavirus RNA. In: Sonenberg N, Hershey JWB and Mathews MB (editors). *Translational Control of Gene Expression Monograph 39*. Cold Spring Harbor, NY: Cold Spring Harbor Laboratory; 2000. pp. 869–900.
12. **Belsham GJ, Brangwyn JK.** A region of the 5′ noncoding region of foot-and-mouth disease virus RNA directs efficient internal

initiation of protein synthesis within cells: involvement with the role of L protease in translational control. *J Virol* 1990;64:5389–5395.

13. Belsham GJ, Mcinerney GM, Ross-Smith N. Foot-and-mouth disease virus 3C protease induces cleavage of translation initiation factors eIF4A and eIF4G within infected cells. *J Virol* 2000;74:272–280.

14. Strong R, Belsham GJ. Sequential modification of translation initiation factor eIF4GI by two different foot-and-mouth disease virus proteases within infected baby hamster kidney cells: identification of the 3C^{pro} cleavage site. *J Gen Virol* 2004;85:2953–2962.

15. Hollister JR, Vagnozzi A, Knowles NJ, Rieder E. Molecular and phylogenetic analyses of bovine rhinovirus type 2 shows it is closely related to foot-and-mouth disease virus. *Virology* 2008;373:411–425.

16. Hinton TM, Ross-Smith N, Warner S, Belsham GJ, Crabb BS. Conservation of L and 3C proteinase activities across distantly related aphthoviruses. *J Gen Virol* 2002;83:3111–3121.

17. de Los Santos T, Diaz-San Segundo F, Grubman MJ. Degradation of nuclear factor kappa B during foot-and-mouth disease virus infection. *J Virol* 2007;81:12803–12815.

18. Wang D, Fang L, Li P, Sun L, Fan J et al. The leader proteinase of foot-and-mouth disease virus negatively regulates the type I interferon pathway by acting as a viral deubiquitinase. *J Virol* 2011;85:3758–3766.

19. Guarné A, Tormo J, Kirchweger R, Pfistermueller D, Fita I et al. Structure of the foot-and-mouth disease virus leader protease: a papain-like fold adapted for self-processing and eIF4G recognition. *EMBO J* 1998;17:7469–7479.

20. Roberts PJ, Belsham GJ. Identification of critical amino acids within the foot-and-mouth disease virus leader protein, a cysteine protease. *Virology* 1995;213:140–146.

21. Piccone ME, Zellner M, Kumosinski TF, Mason PW, Grubman MJ. Identification of the active-site residues of the L proteinase of foot-and-mouth disease virus. *J Virol* 1995;69:4950–4956.

22. Carrillo C, Tulman ER, Delhon G, Lu Z, Carreno A et al. Comparative genomics of foot-and-mouth disease virus. *J Virol* 2005;79:6487–6504.

23. Kirchweger R, Ziegler E, Lamphear BJ, Waters D, Liebig HD et al. Foot-and-mouth disease virus leader proteinase: purification of the Lb form and determination of its cleavage site on eIF-4 gamma. *J Virol* 1994;68:5677–5684.

24. Zamora M, Marissen WE, Lloyd RE. Multiple eIF4GI-specific protease activities present in uninfected and poliovirus-infected cells. *J Virol* 2002;76:165–177.

25. Piñeiro D, Ramajo J, Bradrick SS, Martínez-Salas E. Gemin5 proteolysis reveals a novel motif to identify L protease targets. *Nucleic Acids Res* 2012;40:4942–4953.

26. Schlick P, Kronovetr J, Hampoelz B, Skern T. Modulation of the electrostatic charge at the active site of foot-and-mouth-disease-virus leader proteinase, an unusual papain-like enzyme. *Biochem J* 2002;363:493–501.

27. Glaser W, Cencic R, Skern T. Foot-and-mouth disease virus leader proteinase: involvement of C-terminal residues in self-processing and cleavage of eIF4GI. *J Biol Chem* 2001;276:35473–35481.

28. Fuerst TR, Niles EG, Studier FW, Moss B. Eukaryotic transient-expression system based on recombinant vaccinia virus that synthesizes bacteriophage T7 RNA polymerase. *Proc Natl Acad Sci USA* 1986;83:8122–8126.

29. Belsham GJ, Nielsen I, Normann P, Royall E, Roberts LO. Monocistronic mRNAs containing defective hepatitis C virus-like picornavirus internal ribosome entry site elements in their 5 untranslated regions are efficiently translated in cells by a cap-dependent mechanism. *RNA* 2008;14:1671–1680.

30. Snowdon WA. Growth of FMDV in monolayer cultures of calf thyroid cells. *Nature* 1966;210:1079–1080.

31. Foeger N, Glaser W, Skern T. Recognition of eukaryotic initiation factor 4G isoforms by picornaviral proteinases. *J Biol Chem* 2002;277:44300–44309.

32. Foeger N, Kuehnel E, Cencic R, Skern T. The binding of foot-and-mouth disease virus leader proteinase to eIF4GI involves conserved ionic interactions. *FEBS J* 2005;272:2602–2611.

33. Ohlmann T, Pain VM, Wood W, Rau M, Morley SJ. The proteolytic cleavage of eukaryotic initiation factor (eIF) 4G is prevented by eIF4E binding protein (PHAS-I; 4E-BP1) in the reticulocyte lysate. *EMBO J* 1997;16:844–855.

34. Aumayr M, Fedosyuk S, Ruzicska K, Sousa-Blin C, Kontaxis G et al. NMR analysis of the interaction of picornaviral proteinases Lb and 2A with their substrate eukaryotic initiation factor 4GII. *Protein Sci* 2015;24:1979–1996.

35. Steinberger J, Kontaxis G, Rancan C, Skern T. Comparison of self-processing of foot-and-mouth disease virus leader proteinase and porcine reproductive and respiratory syndrome virus leader proteinase nsp1α. *Virology* 2013;443:271–277.

36. Cencic R, Mayer C, Juliano MA, Juliano L, Konrat R et al. Investigating the substrate specificity and oligomerisation of the leader protease of foot and mouth disease virus using NMR. *J Mol Biol* 2007;373:1071–1087.

37. Chinsangaram J, Piccone ME, Grubman MJ. Ability of foot-and-mouth disease virus to form plaques in cell culture is associated with suppression of alpha/beta interferon. *J Virol* 1999;73:9891–9898.

38. Ellard FM, Drew J, Blakemore WE, Stuart DI, King AM. Evidence for the role of His-142 of protein 1C in the acid-induced disassembly of foot-and-mouth disease virus capsids. *J Gen Virol* 1999;80:1911–1918.

39. Chen GJ, Qiu N, Karrer C, Caspers P, Page MG. Restriction site-free insertion of PCR products directionally into vectors. *Biotechniques* 2000;28:498–500, 504–505.

40. Polacek C, Gullberg M, Li J, Belsham GJ. Low levels of foot-and-mouth disease virus 3C protease expression are required to achieve optimal capsid protein expression and processing in mammalian cells. *J Gen Virol* 2013;94:1249–1258.

41. Yu Y, Wang H, Zhao L, Zhang C, Jiang Z et al. Fine mapping of a foot-and-mouth disease virus epitope recognized by serotype-independent monoclonal antibody 4B2. *J Microbiol* 2011;49:94–101.

42. Bøtner A, Kakker NK, Barbezange C, Berryman S, Jackson T et al. Capsid proteins from field strains of foot-and-mouth disease virus confer a pathogenic phenotype in cattle on an attenuated, cell-culture-adapted virus. *J Gen Virol* 2011;92:1141–1151.

43. Belsham GJ, Jamal SM, Tjørnehøj K, Bøtner A. Rescue of foot-and-mouth disease viruses that are pathogenic for cattle from preserved viral RNA samples. *PLoS One* 2011;6:e14621.

44. Reed LJ, Muench H. A simple method of estimating fifty percent endpoints. *Am J Hyg* 1938;27:493–497.

45. Reid SM, Grierson SS, Ferris NP, Hutchings GH, Alexandersen S. Evaluation of automated RT-PCR to accelerate the laboratory diagnosis of foot-and-mouth disease virus. *J Virol Methods* 2003;107:129–139.

46. Belsham GJ, Normann P. Dynamics of picornavirus RNA replication within infected cells. *J Gen Virol* 2008;89:485–493.